INDIAN INSTITUTE OF TECHNOLOGY BOMBAY

BACHELOR'S THESIS REPORT

Zero-index Bound states in continuum in simulated photonic crystals

Author:
Mithil Vakde

Supervisor:
Prof. Anshuman Kumar

A thesis submitted in fulfillment of the elective requirements for the degree of B. Tech.

in the

Department of Physics

November 22, 2022

INDIAN INSTITUTE OF TECHNOLOGY BOMBAY

Abstract

Department of Physics

B. Tech.

Zero-index Bound states in continuum in simulated photonic crystals

by Mithil Vakde

This project is a continuation of a previous work where we found possible bound states in the continuum (BICs) by simulating a photocrystal. The goal of this project is to prove that the candidates found in the previous work are BICs using the following method:

- Multipolar decomposition of the eigenmodes corresponding to the potential BIC candidates by calculating the electric field

Acknowledgements

I would like to thank Prof. Anshuman Kumar and Mr. Brijesh Kumar for all the help and support they have given me throughout the project. I have learnt a lot from the two of you and I still have a lot to learn going forward. In addition to this I would like to thank IIT Bombay for presenting me the opportunity to carry out research during my undergraduate years.

Contents

Chapter 1

Introduction

1.0.1 Bound States in the Continuum

Bound States in the Continuum (BICs) are localized waves that coexist with extended waves in the continuum band of quantum mechanical or photonic systems. These are a peculiarity of the mathematics behind photonic systems, and was first predicted based on quantum theory. Physically, they can be thought to have a frequency equal to resonance frequency with its imaginary part 0. (This leads to an infinite Quality factor, which we use later on to identify possible BICs). BICs have interesting applications due to its peculiar properties which have been explored in the literature.

1.0.2 Zero refractive index

Metamaterials with zero refractive index have been explored for its exciting potential applications. However, a major drawback to such applications is that such metamaterials often experience large energy losses. Finding BICs in such materials becomes very important as they experience no losses due to their decoupling from radiative modes in the continuum (localisation)

1.0.3 Software Used

We have used the open source software "Legume" for this entire project, based on Minkov et al., 2020. "Legume" allows us to simulate photonic crystal slabs using the method of guided mode expansion. The implementation is in python, providing us a convenient way to work the results generated by 'legume' for further tasks. The tasks accomplished using legume are:

1. Reproducing the photocrystal with a daisy wheel structure from Minkov et al., 2018
2. Simulating the photonic band structure of its various eigenmodes, calculated using guided mode expansion methods
3. Confirming that the BICs guaranteed by the symmetry of the photocrystal can be made degenerate by tuning parameters
4. Finding potential zero-index BIC candidates using parameter optimisation implemented in the "legume" package
5. Calculating the values of the eletromagnetic fields produced by various modes including the modes corresponding to potential zero-index BIC states

1.0.4 Photocrystal Used

We are using Silicon Nitride (SiN, permittivity = 4) as a material for the photocrystal slab. For the purposes of the simulation, we are not using any upper or lower cladding. While this may be very difficult to produce in real life, we use the fact that such structures can be formed in simulations to our advantage. The goal of this project is only to prove the certain states are zero-index BICs. The lack of cladding provides us with cleaner zero-index BIC candidates, which aids us in our goal.

FIGURE 1.1: The unit cell of the daisy crystal photocrystal (structure created on COMSOL)

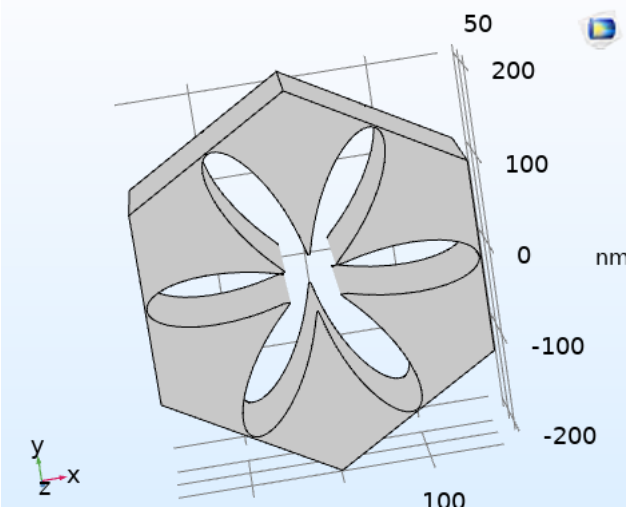

The structure is generated using a discrete Fourier expansion in polar co-ordinates. A general fourier expansions in polar co-ordinates is $r(\phi) = r_0 + \sum(r_n cos(n\phi) + r'_n sin(n\phi))$. For generating the daisy wheel, most coefficients (other than the 0th and 6th coefficients) are set to 0. Giving us 3 tune-able parameters: the thickness of the substrate d and the 2 coefficients of the fourier expansion r_0 and r_d. We use in-built legume methods to search through the parameter space of (d, r_0, r_d). We use "Autograd" to comput gradients and the "lbfgs" minimiser to minimise certain parameters allowing us to find the potential zero-index BIC candidate

1.0.5 Previous Results Used

During the first part of the BTP, we simulated the photocrystal to find BIC candidates using parameters and constraints that would allow us to fabricate and experiment on the crystal in real life. Using the constraints proved to be a difficult task. For this project, we discarded the constraints and tried to find BIC candidates even in photocrystals that would be very difficult to fabricate. This gave us multiple potential candidates.

To start, we used the "visually cleanest" candidate to carry out further calculations. Here we mean that the band structure would visually look like 3 bands crossing each other at a single point, with the middle band being horizontal and the other two bands diagonally crossing each other at the intersection point. Note the triple degeneracy and (approximately) infinite quality factor in the figure below

FIGURE 1.2: Zoom-in of the Photonic Band Structure showing the clean zero index-BIC candidate

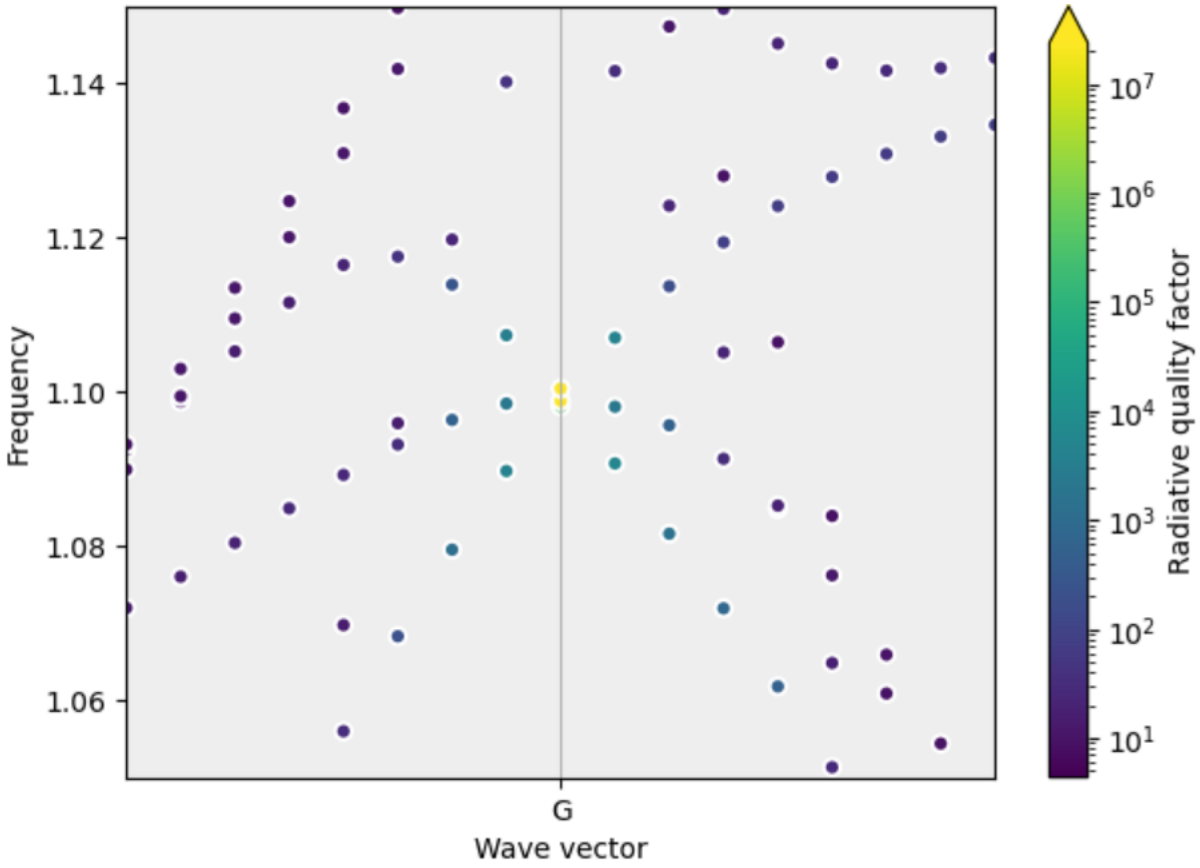

Chapter 2

Multipolar Decomposition

2.0.1 Obtaining the moments

We first take the cleanest potential candidate for zero-index BICs found in the simulations of the SiN photocrystal. The parameters for this candidate are:

$$(d, r_0, r_d) = (0.4, 0.29, 0.21)$$

Then, we find the Electric and magnetic fields for the k-vector corresponding to the frequency where we found the dirac cone. Although ideally, we should be getting a single point of intersection, if we zoom into the band, we see that there are 3 points, very close to each other. Each of these points correspond to a different band. Hence we repeat the following calculations for all three bands. The indices of these bands in our calculations are 14, 15 and 16Here are the electric fields visualised for the three bands:

FIGURE 2.1: Examples showing the x, y and z components of the electric field overlayed on top of the graphic of the daisy wheel structure for (a) band 14

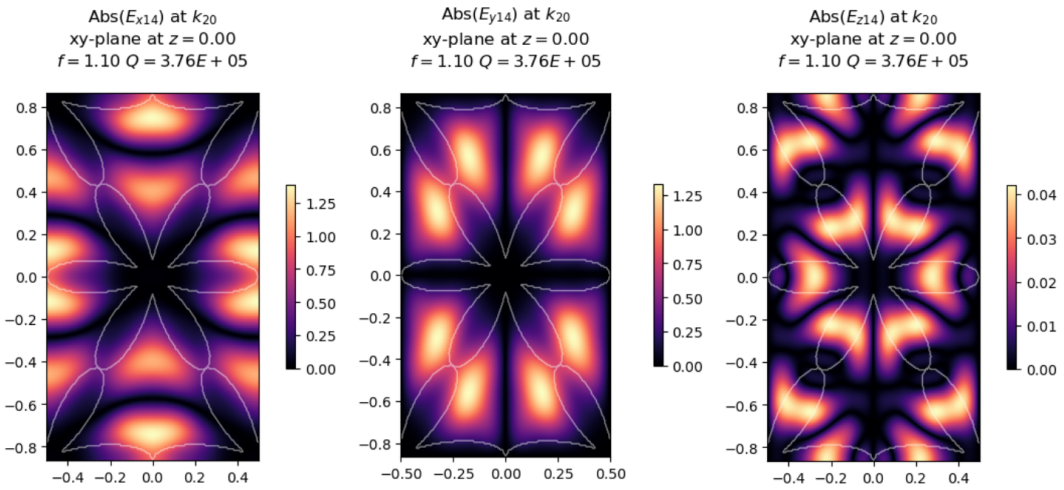

FIGURE 2.2: Examples showing the x, y and z components of the electric field overlayed on top of the graphic of the daisy wheel structure for (b) band 15 and (c) band 16

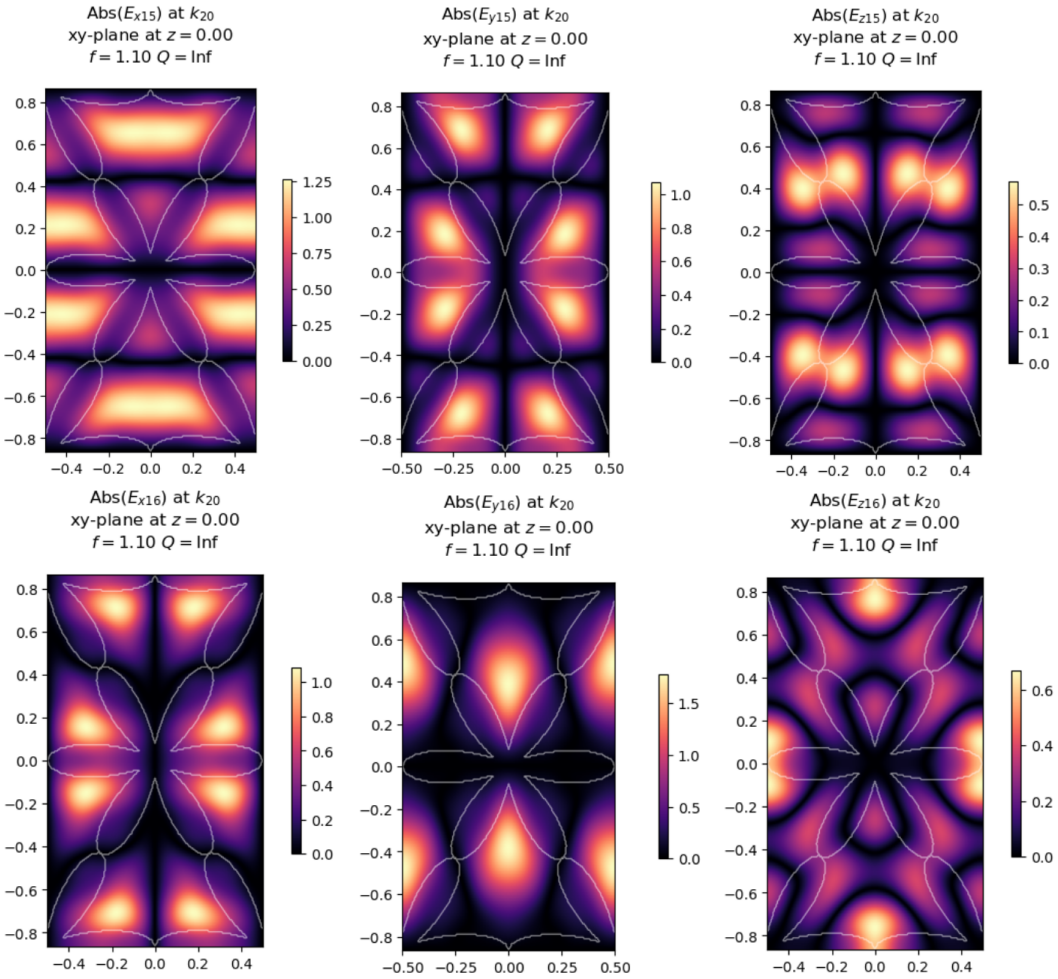

Now we create a cuboidal mask such that it just circumscribes the hexagonal unit cell. To show this works visually, we use the z component of the electric field of the 16th band:

FIGURE 2.3: Applying a cuboidal mask on the unit cell (xy slice)

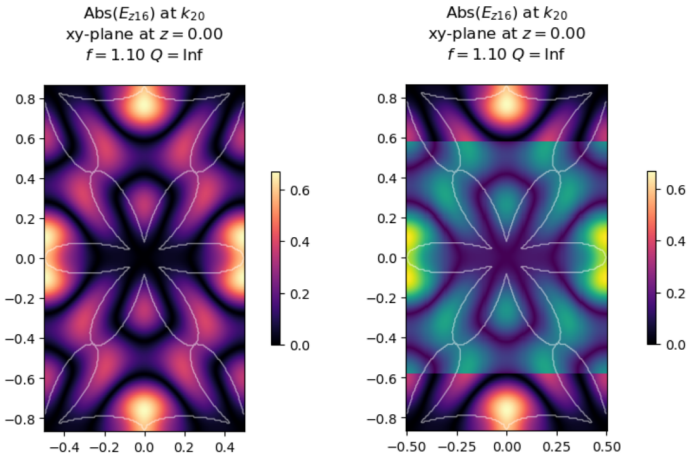

Our goal is to calculate the multipole moments by integrating over one unit cell, and hence the cuboidal mask isn't enough since it overlaps with other unit cells. But the mask allows us to place a hexagonal mesh inside it. This would be harder to place without affixing it to a placeholder like the mask. The reason we place a mesh is to conduct numerical 3D integrals.

FIGURE 2.4: Creating a hexagonal mesh

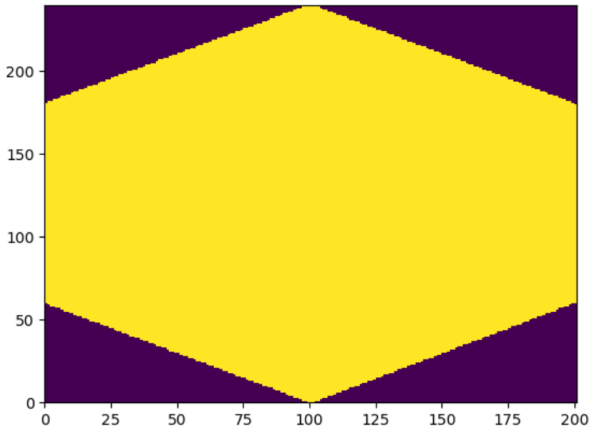

We then apply this mesh onto the previously created mask so that we only include values within the unit cell. The value of the field outside the hexagonal mesh is set to zero
Finally, we can calculate the moments using the following formulae from He et al., 2018:

FIGURE 2.5: Final set up before multipole moments are calculated. A Hexagonal area is selected for integration. The immediate surroundings are set to 0

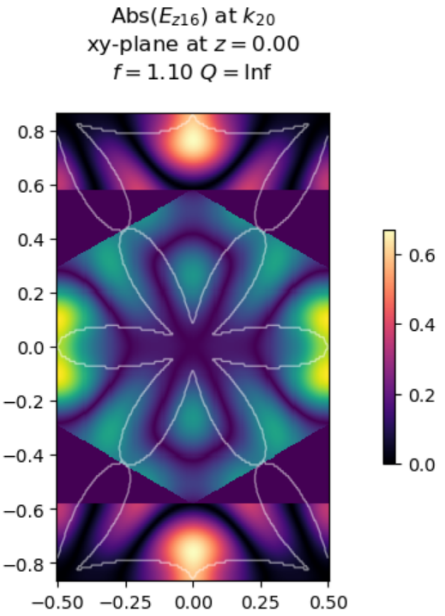

$$P_\alpha = \frac{1}{i\omega}\int d^3 r J_\alpha(\mathbf{r})$$
$$T_\alpha = \frac{1}{10c}\int d^3 r \left[(\mathbf{r}\cdot\mathbf{J}(\mathbf{r}))r_\alpha - 2r^2 J_\alpha(\mathbf{r})\right]$$
$$T^{(1)}_\alpha = \frac{1}{28c}\int d^3 r \left[3r^2 J_\alpha(\mathbf{r}) - 2r_\alpha(\mathbf{r}\cdot\mathbf{J}(\mathbf{r}))r^2\right.$$
$$M_\alpha = \frac{1}{2c}\int d^3 r [\mathbf{r}\times\mathbf{J}(\mathbf{r})]_\alpha$$
$$M^{(1)}_\alpha = \frac{1}{2c}\int d^3 r [\mathbf{r}\times\mathbf{J}(\mathbf{r})]_\alpha r^2$$
$$Q^E_{\alpha,\beta} = \frac{1}{i2\omega}\int d^3 r \left[r_\alpha J_\beta(\mathbf{r}) + r_\beta J_\alpha(\mathbf{r}) - \frac{2}{3}\delta_{\alpha,\beta}(\mathbf{r}\cdot\mathbf{J}(\mathbf{r}))\right]$$
$$Q^M_{\alpha,\beta} = \frac{1}{3c}\int d^3 r \left[(\mathbf{r}\times\mathbf{J}(\mathbf{r}))_\alpha r_\beta + (\mathbf{r}\times\mathbf{J}(\mathbf{r}))_\beta r_\alpha\right]$$
$$Q^T_{\alpha,\beta} = \frac{1}{28c}\int d^3 r \left[4r_\alpha r_\beta(\mathbf{r}\cdot\mathbf{J}(\mathbf{r})) - 5r^2\left(r_\alpha J_\beta + r_\beta J_\alpha\right) + 2r^2(\mathbf{r}\cdot\mathbf{J}(\mathbf{r}))\delta_{\alpha,\beta}\right]$$

We then calculate these values through numerical integration (existing methods are difficult to apply in 3 dimensions for such specific geometries, hence we created our own methods) and plot these values to understand their relative sizes. The absolute values are normalised with respect to the component having the maximum absolute value in each multipole moment. The height of the bar is calculated this way (figures below):

$$[\frac{p_x}{max(p_x,p_y,p_z)}, \frac{p_y}{max(p_x,p_y,p_z)}, \frac{p_z}{max(p_x,p_y,p_z)}, \frac{T_x}{max(T_x,T_y,T_z)}, \ldots]$$

FIGURE 2.6: Multipole moments plotted for each of the 3 bands. Y-axis is normalised separately for dipole(electric magnetic), toroidal, and quadrupole (electric magnetic) moments separately: a) band 14 (b) band 15

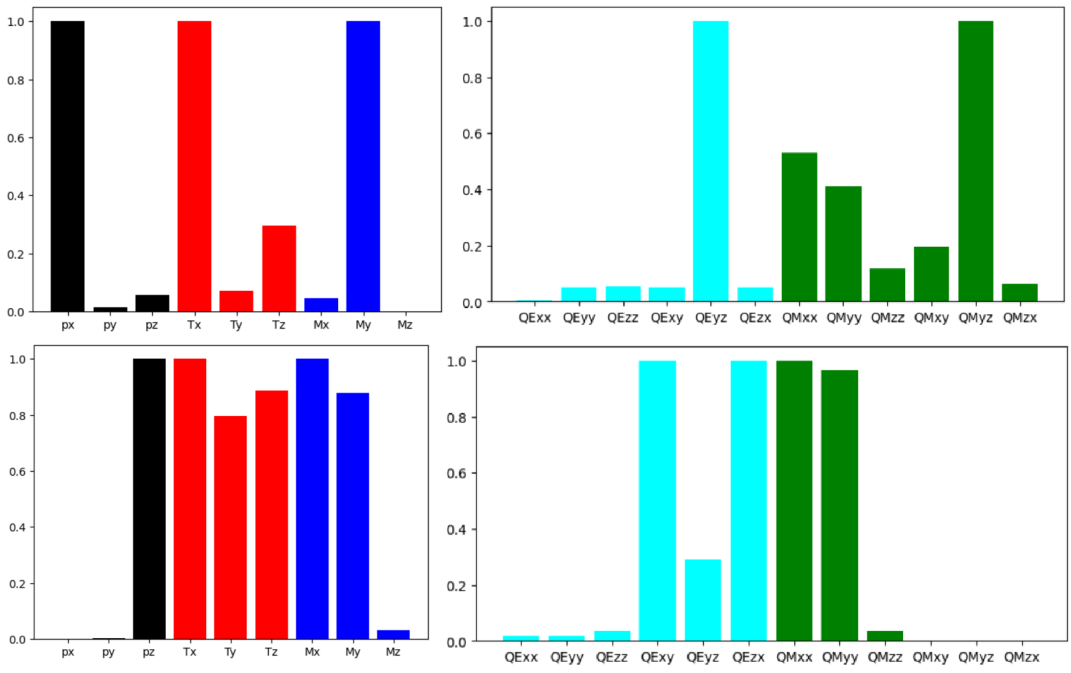

FIGURE 2.7: Multipole moments plotted for each of the 3 bands. The y axis is normalised separately for electric dipole, toroidal, magnetic dipole, electric quadrupoles and magnetic quadrupoles separately: (c) Band 16

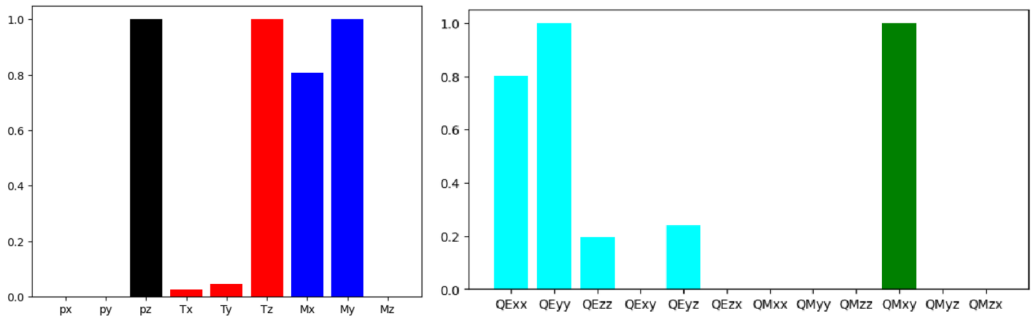

The calculated moments for band 16 are as follows (the values for the other bands are stored here to save space in the report):

$$p_x = 10^{-17} \times (1.066 + i2.003 \times 10^{-7})$$

$$p_y = 10^{-18} \times (-1.300 + i1.646 \times 10^{-8})$$

$$p_z = 10^{-14} \times (1.563 + i3.262 \times 10^{-11})$$

$$T_x = (5.039 \times 10^{-8} - i2.419) \times 10^{-16}$$

$$T_y = (7.008 \times 10^{-9} - i4.243) \times 10^{-16}$$

$$T_z = (2.744 \times 10^{-9} - i8.943) \times 10^{-15}$$

$$M_x = (1.486 \times 10^{-9} - i2.257) \times 10^{-5}$$

$$M_y = (7.270 \times 10^{-10} - i2.790) \times 10^{-5}$$

$$M_z = (7.477 \times 10^{-11} - i1.533) \times 10^{-8}$$

2.0.2 Analysing the Moments

These results can qualitatively prove that the candidate structure we are looking at is a zero-index BIC.

1. Looking at bands 15 and 16, we see that the electric dipoles exists only in the z axis while the magnetic dipoles exist only in the x and y axes. This implies that the propagation of electromagnetic waves occurs only in the X-Y plane for these 2 bands

2. After taking into account the high quality factor at the intersection point, the lack of EM waves propagating along the z axis tells us that band 15 and 16 correspond to bound states in the continuum

3. Looking at band 14, we see that the electric dipole exists only along the x axis while the magnetic dipole exists only in the y axis. This implies that the propagation of electromagnetic waves mainly only along the z axis

4. A careful analysis of the band structure tells us that band 14 corresponds to the horizontal band, which is the zero index band. This doesn't correspond to a bound state in the continuum

5. The triple degeneracy of all these bands at the $\Gamma-$ point gives us very strong evidence that this candidate is indeed a zero-index bound state in the continuum

2.0.3 Other Notes

Using a crystal with these parameters, we have calculated multipole moments. This has taken an unexpectedly large amount of time due to the complexity of the code. Calculating the multipole moments involves manipulations of a number of very large matrices. It would be favourable to carry out such calculations on computing systems that can handle larger scientific computations

The link for the code is here. This can be used for other parameters in the same crystal, and with slight modifications, can be used for other crystals too. The code was made through large changes to the open source "Legume" example code available here.

Chapter 3

Ongoing and Future Work

3.0.1 Verification of multipole decomposition values

While the multipolar decomposition manually calculated seems to match with our expectations, we would like to verify the values using built-in methods in COMSOL. The photocrystal has already been recreated on COMSOL.

3.0.2 Analysing other multipole moments

Our qualitative evidence is based mainly on the dipole moments. We have also calculated the quadrupole and toroidal moments. Analysing these moments can give us further evidence to confirm the candidate is a BIC.

3.0.3 Topological Charges

Recently, the topological nature of BICs has been explored in literature, where they carry conserved and quantised topological charges. These properties would be used to try to obtain quantitative evidence to confirm that the candidates are indeed zero-index BICs

3.0.4 Characterisation of the photocrystal in real life

This would be a 2-step process to perform characterisation of the photocrystal we have used in simulations. First, we are working on creating a setup to image the k-space of any photocrystals on an optical stage. Then we will fabricate the photocrystal with the zero-index BIC and perform characterisation using the set-up

Bibliography

He Yuanand Guo, Guangtao et al. (2018). “Toroidal dipole bound states in the continuum”. en. In: *Physical Review B* 98.16. DOI: 10.1103/physrevb.98.161112. URL: http://dx.doi.org/10.1103/PhysRevB.98.161112.

Minkov, Momchil et al. (2018). “Zero-Index Bound States in the Continuum”. en. In: *Physical Review Letters* 121.26. DOI: 10.1103/physrevlett.121.263901. URL: http://dx.doi.org/10.1103/PhysRevLett.121.263901.

Minkov, Momchil et al. (2020). “Inverse design of photonic crystals through automatic differentiation”. In: *ACS Photonics* 7.7, pp. 1729–1741.

Appendix A

Other References

1. Evlyukhin, Fischer, Reinhardt and Chichkov, PHYSICAL REVIEW B 94, 205434 (2016)
2. Yuan He, Guangtao Guo, Tianhua Feng, Yi Xu, and Andrey E. Miroshnichenko *Supplementary Materials for 'Toroidal Dipole Bound States in the Continuum'*
3. Z. Sadrieva, K. Frizyuk, M. Petrov, Y. Kivshar and A. Bogdanov, arXiv:1903.00309v2 [physics.optics] 20 Apr 2019
4. Bohren and Huffman, *Absorption and Scattering of Light by Small Particles*, Wiley Science Paperback Series, 1988. ISBN 0-471-05772-X
5. Shaimaa I. Azzam and Alexander V. Kildishev, Adv. Optical Mater. 2020, 2001469
6. Thomas Lepetit and Boubacar Kante, PHYSICAL REVIEW B 90, 241103(R) (2014)
7. Legume: Guided Mode Expansion supporting auto-matic differentiation with autograd. https://github.com/ fancompute/legume